

# Detection of Spiculated Lesions in Mammograms

Mehul P. Sampat<sup>1</sup>, Alan C. Bovik<sup>2</sup>

<sup>1</sup>Dept. of Biomedical Engineering, The University of Texas at Austin, TX 78712-1084, USA

<sup>2</sup>Dept. of Electrical and Computer Engineering, The University of Texas at Austin, TX 78712-1084, USA

*Abstract*— In this paper, we present a new technique for the detection of spiculated masses in digitized mammograms. The technique consists of two stages, enhancement of spiculations followed by the detection of the location where they converge. We describe a new algorithm for the enhancement and a new set of linear image filters which we have created for the detection stage. We have tested the algorithm on digitized mammograms obtained from the Digital Database for Screening Mammography (DDSM). Results of the detection algorithm are shown. Finally we show that the algorithm may be modified for the detection of architectural distortions.

*Keywords*— Mammography, Radial Spiculation Filters, Spiculated Masses, Architectural Distortions, Radon Transform, Fast Slant Stack.

## I. INTRODUCTION

The American Cancer Society estimates that in 2003, 211,300 women will be affected by breast cancer and 39,800 will die due to it [1]. Early detection of cancer helps save lives and screening mammography is the most effective tool for early detection of breast cancer [1]. Screening Mammography involves the detection of abnormalities like lesions which are characterized by their shape and margin. Spiculated lesions are highly suspicious signs of breast cancer [2]. By definition, a spiculated lesion is characterized by lines (or spiculations) radiating from the margins of the mass [3].

In this paper, we propose a new algorithm for the detection of spiculated masses in digitized mammograms. The algorithm consists of two steps. Enhancement of certain features using a new filtering algorithm followed by detection of the enhanced features using a novel set of linear filters called Radial Spiculation Filters.

The filtering algorithm aims to enhance the linear features of masses called spiculations. This is done by computing the radon transform of the image, followed by filtering and thresholding in the radon domain and computing an inverse radon transform to obtain the enhanced image. The Radial Spiculation filters are designed to find the spatial location where the spiculations converge. The organization of the paper is as follows: Section II describes the theory of the filtering algorithm and the new set of filters called Radial Spiculation Filters. The methodology and the data sets are described in Section III. Section IV presents the results and the conclusion is described in Section V.

## II. THEORY

In this section, the two steps of the algorithm, Enhancement and Detection are described in detail.

### A. Enhancement of Spiculations

The radon transform of a continuous function  $f(x, y)$  is defined as [4]:

$$\check{g}(\rho, \theta) = \int_{-\infty}^{\infty} \int_{-\infty}^{\infty} f(x, y) \delta(\rho - x \cos(\theta) - y \sin(\theta)) dx dy$$

An image can be viewed as the function  $f(x, y)$  which depends on the spatial coordinates  $(x, y)$ . An important property of the radon transform is that a line in an image is mapped to a point in the radon domain. Figure 1 shows two images and portions of the radon transforms of the images. We note that lines are characterized by ‘Low High Low’ patterns (where Low corresponds to a low magnitude value and High corresponds to a high magnitude value). Thus to detect lines on the image we perform linear filtering in the radon domain. Assuming the columns represent different values of  $\theta$  and rows represent different values of  $\rho$ , we filter the columns of  $\check{g}(\rho, \theta)$  with a column filter like  $[-1 \ 2 \ -1]^T$  to detect lines. We then threshold the radon domain and compute the inverse radon transform to obtain the enhanced image.

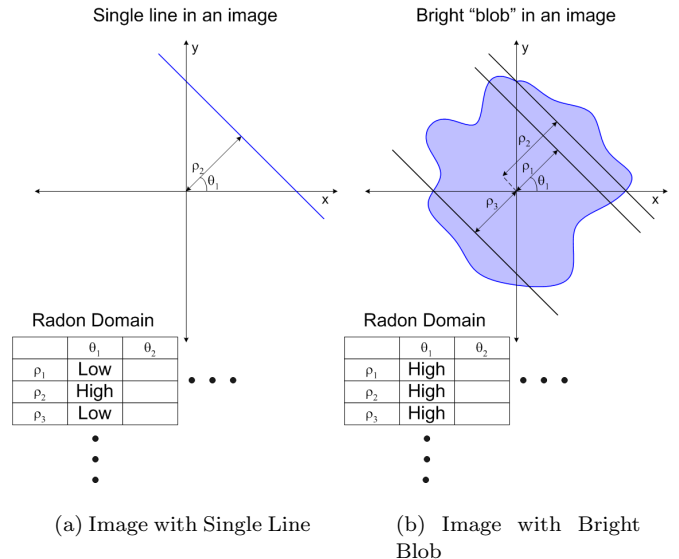


Fig. 1. Radon Examples

### A.1 Summary of the enhancement algorithm

1. Compute the radon transform of the image.
2. Filter the radon domain with a column filter to detect ‘Low High Low’ patterns.
3. Apply a threshold to the filtered radon domain.
4. Compute the inverse radon transform of the image to obtain the enhanced image.

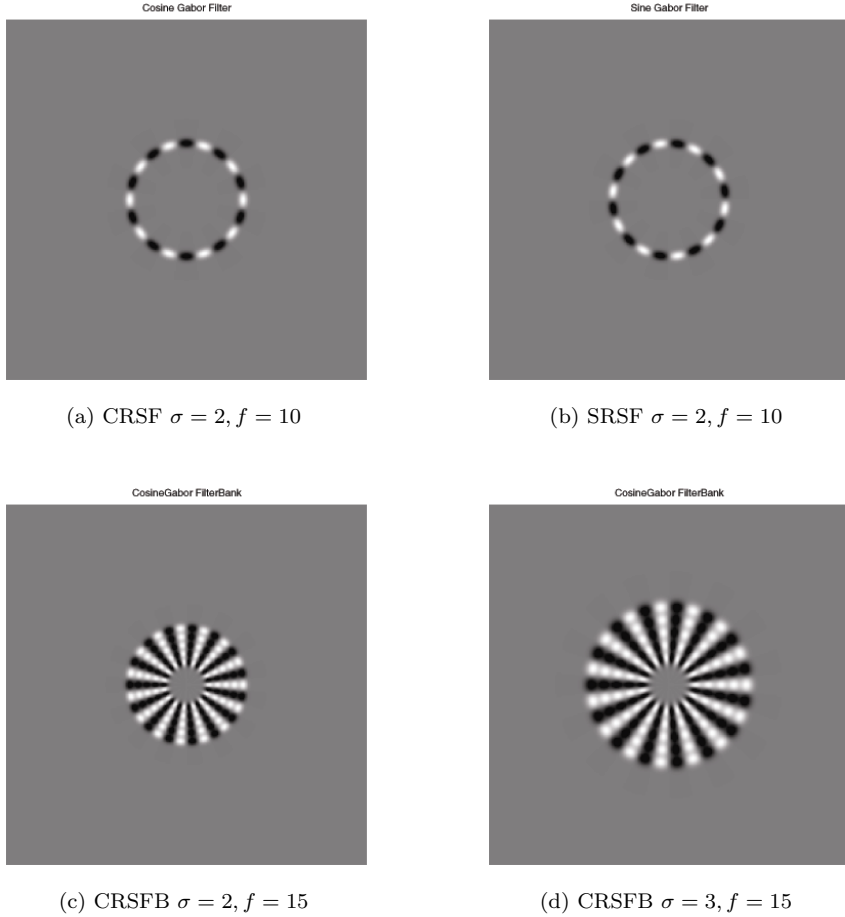


Fig. 2. Radial Spiculation Filters

### B. Detection Using Radial Spiculation Filters

We have invented a new class of linear image filters called Radial Spiculation filters(RSF), which are designed specifically for detecting spiculated masses. They do so by detecting the spatial location where the spiculations converge. We define two types of RSF called, the Cosine Radial Spiculation Filters(*CRSF*) and Sine Radial Spiculation Filters(*SRSF*), defined as:

$$CRSF = g(r_0, \sigma) * \cos(\theta * f) \quad (1)$$

$$SRSF = g(r_0, \sigma) * \sin(\theta * f) \quad (2)$$

$$g(r_0, \sigma) = \exp(-(r - r_0)^2 / (2 * \sigma^2)) \quad (3)$$

Where

$$r = \sqrt{x^2 + y^2}$$

$$\theta = \arctan(y/x)$$

$\sigma$  is the standard deviation in pixels.

$r_0$  is a size parameter in pixels.

$f$  is the frequency in cycles per circumference.

A CRSF and SRSF (with same parameter values of  $\sigma, f, r_0$ ) form a pair of filters. We define a Cosine Spiculation Filter Bank (CRSFB) as a set of CRSF's with same values of  $\sigma$  and frequency  $f$  and with increasing values of  $r_0$ . Any number of CRSF could be used in a CRSFB. For this work

we use 5 in each CRSFB. A corresponding Sine Spiculation filter bank (SRSFB) can be defined similarly. The value of  $r_0$  is increased so that the filters of a bank intersect at half-peak. We now describe how a CRSFB and its corresponding SRSFB can be used for the detection of masses.

#### B.1 Detection Algorithm

1. Construct a CRSFB and the corresponding SRSFB.
2. Filter the enhanced image, obtained after the enhancement stage, with a pair of filters from the two filter-banks.
3. Compute the point-wise root mean square combination of the two filtered images. Let this be the output of the pair of filters.
4. Repeat steps 2 and 3 for each pair of filters from the two banks.
5. Perform a point-wise addition of the outputs of all of the pairs of filters. This is the output of a filter-bank.
6. Find the maxima in the output of the filter-bank. The location of this maxima is marked as the site of the spiculated mass. This is marked with a red colored marker in the results, shown in Figure 5.
7. There maybe more than one mass in a mammogram. To find other possible masses we do the following
8. A circular region (whose center is the location of the

first maxima and whose radius equal to that of the largest mass possible) is set to zero in the output of the filter-bank. 9. The maxima is found in this new image and marked as the site of the second mass. This is marked with a green marker in the results, shown in Figure 5.

10. Similarly we also find the third maxima and mark it as the site of the third mass. This is marked with a blue colored marker in the results, shown in Figure 5.

11. Construct different filter-banks, by varying the parameters  $f$  and  $\sigma$  and repeat steps 2 to 10 for each filter-bank.

### III. METHODOLOGY

We obtained mammograms from the USF Digital Database for Screening Mammography(DDSM) [5]. The images were decimated by a factor of 4. They were then enhanced by the algorithm described in Section II. Recently Averbuch et.al. have defined the Fast Slant Stack transform which is a new definition of a digital radon transform for digital images [6].

To compute the radon transform and the inverse radon transform we used the Fast Slant Stack Transform. The BEAMLAB 200 program was used to compute these transforms. It can be downloaded from <http://www-stat.stanford.edu/~beamlab/>. For thresholding the data in the radon domain a threshold value was selected empirically and the same threshold value was used for all images. The enhanced images were then fed to the detection algorithm defined in section II.

For the detection algorithm we defined CRSFB and SRSFB's at 3 scales ( $\sigma = 1, 2, 3$ ) pixels. At each scale we constructed filter-banks of 5 different frequencies  $f = 5, 10, 15, 20, 25$  cycles per diameter. Thus we had a total of 15 CRSFB's and 15 SRSFB's each consisting of 5 CRSF's and SRSF's respectively. The enhanced image was filtered was all of the 15 filter banks and a single output was generated for each filter-bank pair as described in Section II. The output of all of the filter-banks at a scale were combined to generate one output per scale. Thus a total of 3 output's were generated. The first, second and third maxima were found on each of these outputs as described in Section II. These are marked as the center of the spiculated masses.

### IV. RESULTS

The results of the detection algorithm are shown in Figures 3, 4 and 5. We show the results of the algorithm on 3 different mammograms. Figure 3(a) shows a thumbnail of the original image with the ground truth overlaid on it in red. The spiculated mass has been circled in red by a radiologist. This thumbnail was also obtained from the DDSM database. Figure 3(b) shows the cropped original image while figure 3(c) show the results obtained after the enhancement algorithm.

This enhanced image is passes through the detection algorithm described in section II-B and location of the spiculated mass is detected. In figure 3(d) this location is marked on the original image with a red marker. Note

that a Region of interest (ROI) containing the mass can now be selected automatically for further processing like classification of lesions.

Similarly the results for another mammogram are shown in 4. The thumbnail in Figure 4(a) shows the spiculated mass encircled in red and the results of enhancement and detection are shown in Figure 4(c) and 4(d) respectively. By design, this algorithm is well suited to detect another sign of cancer known as an Architectural Distortion. This is characterized by spiculations radiating from a point and focal retraction or distortion of the edge of the parenchyma [3]. The mammogram shown in Figure 5 contains an Architectural Distortion. The results in Figures 5(c) and 5(d) show that it was detected accurately.

Other authors have previously developed algorithms for the detection of spiculated masses in mammograms [7–12]. However it is difficult to compare the different algorithms as they were applied on images from different databases. Also very little work has been done for the detection of architectural distortions.

### V. CONCLUSION

A new technique for the detection of spiculated lesions was presented. Promising results were obtained with our preliminary experiments. Further testing of the algorithm is currently under-way. It was shown that the algorithm could be extended for the detection of architectural distortions.

### REFERENCES

- [1] ACS, "American Cancer Society: Cancer Facts and Figures 2003," Tech. Rep., American Cancer Society, Atlanta, Ga, 2003.
- [2] D.B. Kopans, *Breast Imaging*, Lippincott Williams, 2nd edition, January 1998.
- [3] American College of Radiology(ACR), *Illustrated Breast Imaging Reporting and Data System(BI-RADS<sup>TM</sup>)*, Reston[VA]: American College of Radiology, third edition, 1998.
- [4] A. C. Bovik, *Handbook of Image and Video Engineering*, Academic Press, first edition, 2000.
- [5] M. Heath, K.W. Bowyer, and D. Kopans, "Current status of the digital database for screening mammography," *Digital Mammography*, pp. 457–460, 1998.
- [6] A. Averbuch, R.R. Coifman, D.L. Donoho, M. Israeli, and J. Walden, "A notion of radon transform for data in a cartesian grid which is rapidly computible, algebraically exact, geometrically faithful and invertible," 2001.
- [7] N. Karssemeijer and G. M. Brake, "Detection of stellate distortions in mammograms," *IEEE Transactions on Medical Imaging*, vol. 15, no. 5, 1996.
- [8] S. L. Liu, C. F. Babbs, and E. J. Delp, "Multiresolution detection of piculated lesions in digital mammograms," *IEEE Transactions on Image Processing*, vol. 10, no. 6, 2001.
- [9] H. Kobatake and Y. Yoshinaga, "Detection of spicules on mammogram based on skeleton analysis," *IEEE Transactions on Medical Imaging*, vol. 15, no. 5, 1996.
- [10] Huai Li, Yue Wang, K. J. Ray Liu, Shih-Chung B. Lo, and Matthew T. Freedman, "Computerized radiographic mass detection part I: Lesion site selection by morphological enhancement and contextual segmentation," *IEEE Transactions on Medical Imaging*, vol. 20, no. 4, pp. 289–301, April 2001.
- [11] G. M. Brake and N. Karssemeijer, "Single and multiscale detection of masses in digital mammograms," *IEEE Transactions on Medical Imaging*, vol. 18, no. 7, pp. 628–639, July 1999.
- [12] H. Kobatake, M. Murakami, H. Takeo, and S. Nawano, "Computerized detection of malignant tumors on digital mammograms," *IEEE Transactions on Medical Imaging*, vol. 18, no. 5, 1999.

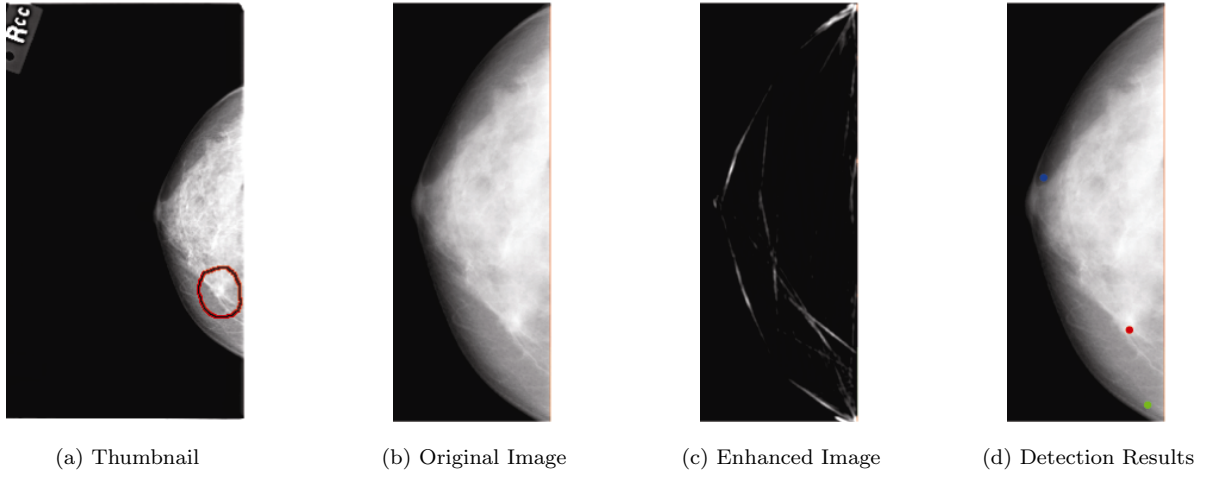


Fig. 3. Mammogram with Spiculated Lesion

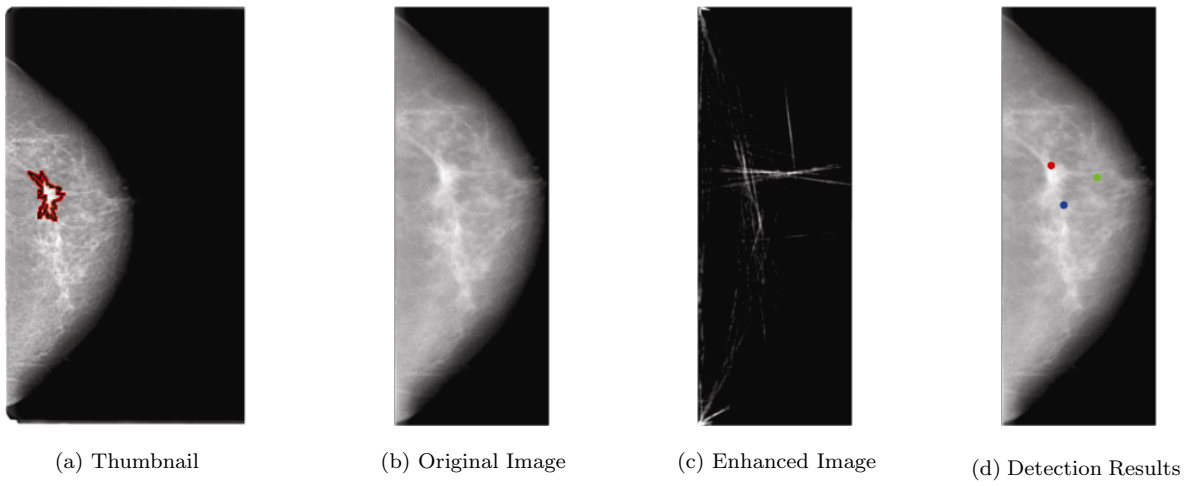


Fig. 4. Mammogram with Spiculated Lesion

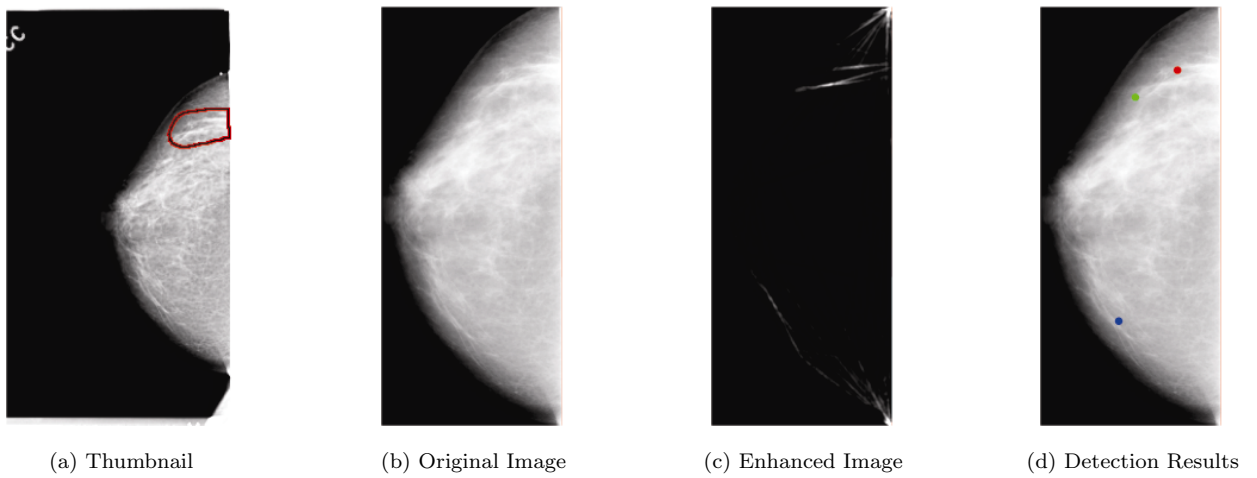


Fig. 5. Mammogram with Architectural Distortion